Article

Application of Landsat Imagery to Investigate Lake Area Variations and Relict Gull Habitat in Hongjian Lake, Ordos Plateau, China

Kang Liang [1],* and Guozhen Yan [2]

[1] Key Laboratory of Water Cycle and Related Land Surface Processes, Institute of Geographic Sciences and Natural Resources Research, Chinese Academy of Sciences, Beijing 100101, China

[2] College of Forestry, Beijing Forestry University, Beijing 100083, China; ygzh4161@163.com

* Correspondence: liangk@igsnrr.ac.cn; Tel.: +86-10-64889671

Abstract: Lakes in arid and semi-arid regions have an irreplaceable and important role in the local environment and wildlife habitat protection. Relict Gull (*Larus relictus*), which is listed as a "vulnerable" bird species in the IUCN Red List, uses only islands in lakes for habitat. The habitat with the largest colonies in Hongjian Lake (HL), which is located in Shaanxi Province in China, has been severely threatened by persistent lake shrinkage, yet the variations in the area of the lake and the islands are poorly understood due to a lack of in situ observations. In this study, using the Modified Normalized Difference Water Index, 336 Landsat remote sensing images from 1988–2015 were used to extract the monthly HL water area and lake island area, and the driving factors were investigated by correlation analysis. The results show that the lake area during 1988–2015 exhibited large fluctuations and an overall downward trend of -0.94 km^2/year, and that the lake area ranged from 55.02 km^2 in 1997 to 30.90 km^2 in 2015. The cumulative anomaly analysis diagnosed the lake variations as two sub-periods with different characteristics and leading driving factors. The average and change trend were 52.88 and 0.21 km^2/year during 1988–1998 and 38.85 and -1.04 km^2/year during 1999–2015, respectively. During 1988–1998, the relatively high precipitation, low evapotranspiration, and low levels of human activity resulted in a weak increase in the area of HL. However, in 1999–2015, the more severe human activity as well as climate warming resulted in a fast decrease in the area of HL. The variations in lake island area were dependent on the area of HL, which ranged from 0.02 km^2 to 0.22 km^2. As the lake size declined, the islands successively outcropped in the form of the four island zones, and the two zones located in Northwest and South of HL were the most important habitats for Relict Gull. The formation of these island zones can provide enough space for Relict Gull breeding.

Keywords: lake area; island; *MNDWI*; climate change; Relict Gull(*Larus relictus*); Hongjian Lake

1. Introduction

Lakes in arid and semi-arid regions, despite covering only a small fraction of the landscape, have an irreplaceable role and special significance for local human inhabitants, animals, and plants and serve to protect living hydrological and ecological environments [1,2]. As sensitive and good indicators of changing environments at both regional and global scales [3–7], lakes have long been an academic focus. The variations in lake area and lake water levels and the responses to climate change and intensifying anthropogenic activities have been widely investigated all over the world in recent years [8–13]. For lakes widely distributed across ungauged basins (i.e., those lacking meteorological and hydrological stations) and in remote and poor regions, it is very difficult to quantify lake dynamics and the causes of variations. However, for this challenge, with the rapid development of remote

sensing technology, direct monitoring lake dynamics using multi-source remote sensing data is more convenient and widely used in such poorly observed basins [14–19].

Relict Gull (*Larus relictus*) is a bird species unique to arid and semi-arid ecological regions. It has been classified as a "vulnerable" species on the IUCN Red List (http://www.iucnredlist.org) since 2000 because the population of this gull is restricted to breeding only at a small number of islands in saline and slightly saline lakes located in arid regions that could be strongly influenced by climate changes and human interference [20]. The stability of lake and lake islands is an essential condition for Relict Gull's survival and reproduction. No nesting takes place if lakes dry up, if the islands become joined to the shore, or if the islands become too small due to water-levels being too high [20–23]. Hongjian Lake, located in Shaanxi Province, China, has played a key role in saving and supporting the largest colonies of Relict Gull since 2003 [20,24]. Studies about changes to Hongjian Lake and the lake islands and the reasons for these changes are very important and necessary for the protection of lake wetland and Relict Gull's habitat.

Existing studies about Hongjian Lake have mainly focused on zoology [24–27], records of environmental evolution [28–30], and landscape changes [31–33]. Hongjian Lake is located in a typical ungauged basin, and its long-term hydrologic process changes and the causes of these changes are difficult to monitor without hydrological or meteorological in situ data. Some researchers have attempted to analyze the basic hydrologic conditions of Hongjian Lake, including the water balance [34–36], ecological water demand [34], water quality variations 29 September 2017 [37], and lake size variations [37–42]. Especially for the lake size variations, remote sensing technology is powerful and convenient for monitoring long-term changes. Specifically, MODIS imagery and the MOD13Q1 vegetation index product with a 250-m resolution were used to obtain the water area of Hongjian Lake after 2000 [38,39,42]. Landsat imagery with a higher-resolution (60 m and 30 m) was also used to monitor the annual lake area in some different representative periods [37,40,41,43]. This research generally revealed that the water area of Hongjian Lake exhibited severe shrinkage, and discussed the driving factors behind the shrinkage including climate change (i.e., precipitation, temperature or evapotranspiration) and anthropogenic disturbances (e.g., human direct water usage for irrigation, industry, and domestic uses). However, due to the limitations of the relatively coarse resolution (250 m) and the starting date (only after 2000) of MODIS, the potentially insufficient representativeness of choosing only one image from Landsat or MODIS imagery in some month as being representative of the whole year, the relatively coarse change processes described by some Landsat or MODIS imagery in only a few representative years, as well as the difficulty of acquiring data of human driving factors, the more detailed variations in this lake's hydrologic process and a comprehensive analysis of the drivers behind these changes have not been quantitatively explored in depth. Moreover, the previous research paid little attention to the changes in the lake islands (i.e., Relict Gull habitat), and no further quantitative analysis has been conducted to investigate variations in the lake islands and the relationships between island variations and the Relict Gull population. Based on Landsat imagery with a 30 m-resolution and quantifiable data on driving factors during 1988–2015, our study aims to investigate the variations in lake area, to identify the characteristics of and changes in the Relict Gull's habitat, to analyze the driving factors behind lake variations, and to provide some advice and implications for the protection of lake wetland and Relict Gull.

2. Materials and Methods

2.1. Study Site

Hongjian Lake (HL), belonging to Shenmu County, serves as the boundary between the Inner Mongolia Autonomous Region and Shaanxi Province, China (Figure 1). HL is the largest desert freshwater lake in China [34] and is currently the largest Relict Gull breeding ground and habitat in the world [20,24]. HL is an irregular triangle-shaped lake, and it is recorded that the lake, with an area of only 1.3 km^2, formed in approximately 1929 due to the increase in precipitation in

the early 20th century [28]. HL expanded gradually to 20 km^2 in 1947, and then, the lake quickly enlarged to 40 km^2 in 1958 because of artificial dredging. In the mid-1990s, the lake surface area was 60.3 km^2, with a maximum water depth of 10.5 m and an average water depth of 8.2 m [28,38]. HL was officially recognized as a provincial scenic spot in 1995 and was then upgraded to a national 4A-level scenic spot in 2012. The HL wetland was classified as a nature reserve at the county level in 1996 and was then upgraded to a provincial-level nature reserve in 2014. In addition, HL was listed as an important wetland in the "Chinese Wetland Protection Motion Plan" in 2000 and was then simultaneously included in the list of important wetlands in Shaanxi Province and the list of important wetlands in China in 2008.
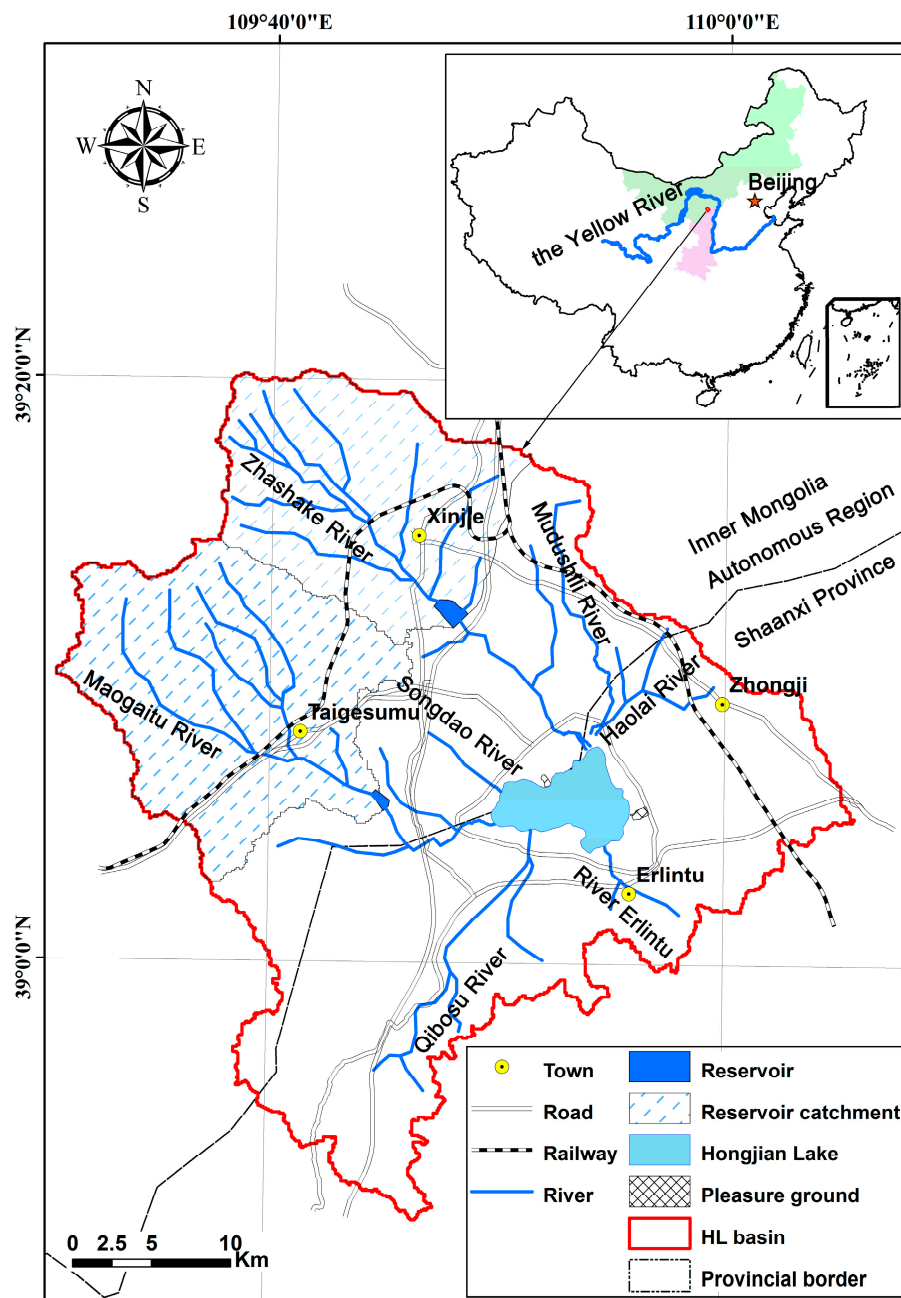

Figure 1. A map of the Hongjian Lake basin (HL basin).

HL is in a naturally closed basin (38°51′10″–39°20′20″N, 109°30′38″–110°5′46″E) with a drainage area of 1352 km^2 and an elevation of 1200–1417 m. Seven seasonal rivers flow into the lake:

the Mudushili River, the Zhashake River, the Maogaitu River, the Songdao River, the Haolai River, the Qibosu River, and the Erlintu River, none of which have any hydrometric stations [39]. The Zhashake Reservoir and the Maogaitu Reservoir, which are located along the Zhashake River and the Maogaitu River (Figure 1), were built in 2005 and 2009 [44], and have catchment areas of 227 km^2 and 284 km^2, respectively. HL is mainly supplied by the above seven inflowing rivers, precipitation and groundwater, and the lake has no outflows [28]. The HL basin is under a typical temperate continental semiarid monsoon climate with distinct seasonal variations, including drought in spring, warm summers, dry autumns, and cold winters. The average annual temperature from 1973 to 2015 was 7.2 °C. The average temperature in the hottest month, July, is 22.2 °C, while that in the coldest month, January, is −10.1 °C. The average annual precipitation from 1973 to 2015 in the HL basin was approximately 376.5 mm, and precipitation is mainly concentrated from June to September, accounting for 77% of the annual precipitation. Grassland, sand land, woodland, cropland and lake water surface are the main land use types in the HL basin [33]. Grassland and shrubs are the primary vegetation types in the HJ basin. There are four towns in the HL basin, including Xinjie Town and Taigesumu Town in the Inner Mongolia Autonomous Region, and Zhongji Town and Erlintu Town in Shaanxi Province (Figure 1).

HL has played a key role in saving and sustaining most of the Relict Gull's population since 2003. The individuals in Hongjian Lake had been well monitored and documented since 2001 by the Forest Station of Shaanxi Yulin City, ranging from less than 200 in 2001 to over 15,000 in 2010 [24,25]. The IUCN Red List of Threatened Species and BirdLife International [20] make a good introduction to Relict Gull's taxonomy, assessment information, geographic range, population, habitat and ecology. All known breeding colonies of Relict Gull are below 1500 m, in the arid-steppe zone, only on islands in saline and slightly saline lakes with fluctuating waterlevels [20]. Relict Gull breeds at two localities in eastern Kazakhstan [45], one in Russia and several in Mongolia, whilst the largest colonies are thought to occur in China, at Hongjian Lake, Shaanxi [24,25,46] and previously at Bojiang Lake on the Ordos Plateau in Inner Mongolia [23,46,47]. The population is placed in the band for 10,000–19,999 mature individuals, equating to 15,000–29,999 individuals in total. The current population is suspected to be decreasing at a moderate rate, as threats such as the reclamation of wetlands for development, and human disturbance at breeding sites, and instability of breeding areas owing to weather fluctuations and intensive human activities continue to influence most of the range. Loss of ephemeral lake wetland habitats in arid regions, associated with climate change, could greatly affect this species in the near future [20].

2.2. Data

Corresponding to the research aims and the sequence of data usage, four kinds of data were collected in this study: (1) Landsat imagery for extracting the lake surface area and lake islands during 1988–2015; (2) the Relict Gull's population during 2001–2015; (3) three climatic factors (i.e., precipitation, temperature, and potential evapotranspiration); and (4) seven indicators of human activity (i.e., land use types, the Normalized Differential Vegetation Index, human population, sheep population, gross industrial output value, hydraulic engineering construction, and tourism development).

First, Level 1 Terrain-Corrected (L1T) Landsat TM/ETM+and OLI imagery remote sensing data were acquired for extracting the monthly lake surface area and lake islands during 1988–2015. Landsat imagery was downloaded from the United States Geological Survey's (USGS) remote sensing image database (http://earthexplorer.usgs.gov/). In total, 336 Landsat remote sensing images were used in this study, and basic information about this imagery is shown in Table 1. The remote sensing imagery used had clear skies or only slight cloud contamination around the lake regions. Second, data on annual Relict Gull populations in HL during 2001–2015 were acquired from by the Forest Station of Shaanxi Yulin City, and these population data were obtained through the field surveys [24,25].

Table 1. Information on Landsat remote sensing imagery for the HL basin during 1988–2015.

Year	Sensor	Path/Row	Acquisition Date (DD/MM)
1988	TM	127/33	28 January, 29 February, 31 March, 17 April, 19 May, 20 June, 21 July, 07 August, 08 September, 26 October, 27 November, 29 December
1989	TM	127/33	14 January, 15 February, 03 March, 20 April, 22 May, 07 June, 09 July, 26 August, 27 September, 29 October, 30 November, 16 December
1990	TM	127/33	17 January, 18 February, 22 March, 23 April, 25 May, 10 June, 12 July, 29 August, 21 September, 16 October, 17 November, 19 December
1991	TM	127/33	20 January, 21 February, 25 March, 26 April, 28 May, 29 June, 31 July, 30 August, 17 September, 19 October, 20 November, 22 December
1992	TM	127/33	23 January, 24 February, 27 March, 28 April, 30 May, 15 June, 17 July, 18 August, 19 September, 21 October, 22 November, 24 December
1993	TM	127/33	25 January, 26 February, 30 March, 15 April, 17 May, 18 June, 20 July, 05 August, 22 September, 24 October, 25 November, 27 December
1994	TM	127/33	28 January, 13 February, 17 March, 18 April, 20 May, 21 June, 07 July, 24 August, 25 September, 27 October, 28 November, 30 December
1995	TM	127/33	31 January, 16 February, 20 March, 21 April, 07 May, 24 June, 26 July, 27 August, 12 September, 30 October, 15 November, 24 December
1996	TM	127/33	25 January, 19 February, 06 March, 23 April, 25 May, 10 June, 12 July, 29 August, 30 September, 23 October, 24 November, 10 December
1997	TM	127/33	20 January, 21 February, 25 March, 26 April, 28 May, 29 June, 31 July, 16 August, 17 September, 19 October, 20 November, 22 December
1998	TM	127/33	23 January, 24 February, 28 March, 29 April, 31 May, 16 June, 02 July, 19 August, 20 September, 22 October, 24 November, 25 December
1999	TM	127/33	26 January, 27 February, 31 March, 16 April, 18 May, 19 June, 21 July, 22 August, 23 September, 25 October, 26 November, 28 December
2000	TM/ETM+	127/33	22 January, 14 February, 17 March, 18 April, 20 May, 21 June, 23 July, 24 August, 25 September, 27 October, 28 November, 30 December
2001	TM/ETM+	127/33	31 January, 16 February, 20 March, 21 April, 23 May, 24 June, 26 July, 27 August, 28 September, 30 October, 22 November, 17 December
2002	TM/ETM+	127/33	18 January, 19 February, 23 March, 24 April, 26 May, 27 June, 29 July, 30 August, 15 September, 17 October, 18 November, 20 December
2003	TM/ETM+	127/33	21 January, 22 February, 25 March, 27 April, 29 May, 30 June, 17 July, 17 August, 18 September, 20 October, 21 November, 23 December
2004	TM/ETM+	127/33	24 January, 25 February, 28 March, 29 April, 31 May, 16 June, 18 July, 19 August, 20 September, 22 October, 23 November, 25 December
2005	TM/ETM+	127/33	26 January, 27 February, 31 March, 16 April, 18 May, 19 June, 20 July, 22 August, 23 September, 25 October, 26 November, 28 December
2006	TM/ETM+	127/33	29 January, 14 February, 27 March, 19 April, 21 May, 22 June, 24 July, 25 August, 26 September, 28 October, 29 November, 31 December
2007	TM/ETM+	127/33	24 January, 25 February, 21 March, 22 April, 24 May, 25 June, 18 July, 20 August, 21 September, 23 October, 24 November, 26 December
2008	TM/ETM+	127/33	19 January, 20 February, 23 March, 24 April, 26 May, 27 June, 29 July, 30 August, 15 September, 17 October, 18 November, 20 December
2009	TM/ETM+	127/33	21 January, 22 February, 26 March, 27 April, 29 May, 30 June, 24 July, 17 August, 18 September, 20 October, 21 November, 23 December
2010	TM/ETM+	127/33	24 January, 25 February, 26 March, 30 April, 16 May, 17 June, 19 July, 20 August, 21 September, 23 October, 24 November, 26 December
2011	TM/ETM+	127/33	27 January, 28 February, 23 March, 17 April, 19 May, 20 June, 22 July, 23 August, 24 September, 26 October, 22 November, 24 December
2012	ETM+	127/33	22 January, 23 February, 26 March, 27 April, 29 May, 30 June, 16 July, 17 August, 18 September, 20 October, 21 November, 23 December
2013	ETM+/OLI	127/33	24 January, 25 February, 29 March, 30 April, 21 May, 25 June, 27 July, 28 August, 29 September, 23 October, 24 November, 26 December
2014	OLI	127/33	19 January, 20 February, 24 March, 22 April, 24 May, 25 June, 27 July, 31 August, 22 September, 18 October, 19 November, 21 December
2015	OLI	127/33	22 January, 23 February, 27 March, 28 April, 30 May, 15 June, 17 July, 18 August, 19 September, 21 October, 22 November, 24 December

Third, regarding the three climatic factors used in this study, the two meteorological data products (i.e., monthly precipitation and surface air temperature) for 1988–2015 were provided by the China Meteorological Data Service Center (CMDC, http://data.cma.cn/en) with a spatial resolution of $0.5° \times 0.5°$. Potential evapotranspiration (ET_0) in the HL basin was calculated using the Penman–Monteith method recommended by the Food and Agriculture Organization (FAO) (Equation (2) in Section 2.3) [48]. The meteorological elements and variables for calculating ET_0 were obtained from the data from the Yijinhuoluoqi weather station (39°20′24″N, 109°25′48″E), which is the station nearest to the HL basin. These data were provided by the National Climate Center of China Meteorological Administration (CMA). The meteorological data included daily precipitation, air temperatures, wind speed, vapor pressure and sunshine hours.

Lastly, the data for the seven indicators of human activity are from two types of sources. Remote sensing data were used to show the four indicators (i.e., the land use types, Normalized Differential Vegetation Index, hydraulic engineering construction, and tourism development). Land-use and land-cover change (LUCC) datasets with a spatial resolution of 30 m× 30 m in 1990, 1995, 2000, 2010 and 2015 were provided by the Data Center for Resources and Environmental Sciences, Chinese Academy of Sciences (RESDC) (http://www.resdc.cn). The areas of farmland, grassland and woodland are used as proxy indices to indirectly represent irrigation water and vegetation water consumption. The Normalized Differential Vegetation Index (*NDVI*) dataset from the Advanced Very High Resolution Radiometer (AVHRR) Global Inventory Modeling and Mapping Studies (GIMMS) *NDVI* [49] from 1988 to 1999 and the MODIS *NDVI* from 2000 to 2015 were employed as proxy indices to reflect the vegetation changes and vegetation water consumption in the HL basin. The GIMMS *NDVI* dataset has a 8-km spatial resolution with a 15-day interval (https://ecocast.arc.nasa.gov/data/pub/gimms/). The MODIS *NDVI* used is the MOD13Q1 product with a 250-m spatial resolution and a 16-day interval (https://modis.gsfc.nasa.gov/data/dataprod/mod13.php). The maximum value composite (MVC) method [50], which can reduce the impacts of atmospheric clouds, shadows, solar zenith angle and aerosol scattering [51], was used to extract monthly max *NDVI* value of non-water area for the HL basin from GIMMS *NDVI* and MODIS *NDVI* data, and then the values from January to December were averaged to create the average annual *NDVI* for the years of 1988–2015. The two main reservoirs and the main amusement parks and docks in the HL basin were shown using Google Earth images from SPOT5 with a 2.5-m resolution. A Digital Elevation Model (DEM), ASTER GDEM, with a 30 m-resolution for watershed analysis (see Section 2.3.4.) was downloaded from the site (https://earthdata.nasa.gov/). For the socioeconomic data used in this study, the human population (*HP*), sheep population (*SP*), and gross industrial output value (*GIOV*) of the four towns located in the HL basin were used to indirectly represent the domestic water and industrial water usage in the basin. The annual statistical data during 1988–2004 were extracted from reference documents [32], and the annual data during 2005–2013 were provided by the Statistics Bureau of Shenmu County in Shaanxi Province and the Statistics Bureau of Yijinhuoluo County in the Inner Mongolia Autonomous Region. The data for 2014 and 2015 were taken from the China County Statistical Yearbook (Township-Level).

2.3. Methods

Here, corresponding to the research aims and the data used, five types of methods are introduced in this section: (1) extracting lake surface area using the Modified Normalized Difference Water Index; (2) extracting the area of lake islands using artificial visual interpretation; (3) field survey methods to estimate Relict Gull's population; (4) estimation of a climatic factor (potential evaporation) using the Penman–Monteith equation and the determination of reservoirs control areas using watershed analysis; and (5) statistical methods for trend analysis and correlation analysis.

2.3.1. Remote-Sensing Extraction of Lake Surface Area Using the Modified Normalized Difference Water Index

Here, the Modified Normalized Difference Water Index (*MNDWI*) method proposed by Xu [52] is adopted to measure the surface area of Hongjian Lake from Landsat TM/ETM+ and OLI imagery. The *MNDWI* method, a modification of the Normalized Difference Water Index (*NDWI*) [53], has been widely used to extract water bodies [19,23,47,54]. The *MNDWI* is expressed as:

$$MNDWI = \frac{Green - MIR}{Green + MIR} \tag{1}$$

A three-step procedure was used to measure the lake surface area. Step 1 was the calculation of the *MNDWI* according to Equation (1) for all the Landsat images used after pretreatment with a radiation calibration and atmospheric correction. All these processes were accomplished in ENVI 5.1. The radiation calibration was processed using the general tool of Radiation Calibration. The atmospheric correction was processed using the tool of QUick Atmospheric Correction (QUAC). QUAC method, introducing a user-friendly interface, is an in-scene approach to atmospheric correction and determines parameters directly from the information contained within the scene using the observer pixel spectra. The calculations of *MNDWI* were performed using the Band Math tool. Step 2 was the cropping of the HL region by the artificially designated mask. The mask around the lake shore was a little larger than the maximum lake area. Step 3 was the testing and selection of the *MNDWI* threshold. In this study, based on pre-tests, different *MNDWI* threshold values ranging 0.30–0.40 were tested using false color composite reference images by the SWIR2, SWIR1 and green bands. Based on the tests to the specific *MNDWI* threshold value from Landsat TM/ETM+ and OLI imagery in the typical years (i.e., 1988, 1991, 1994, 1997, 2000, 2003, 2006, 2009, 2011, 2013, and 2015) and in different months (i.e., February, April, June, August, October and December), we finally set the *MNDWI* threshold value as 0.35 to segment all the *MNDWI* images (Table 1) into lake water area and non-water area for HL. The *MNDWI* threshold of 0.35 is general for all images in Table 1. Regarding the absolute percent differences in lake area from the various threshold values and our choice of threshold (0.35), we took the images in each month in the two typical years (i.e., 1997 with the maximum annual lake area and 2015 with the minimum annual lake area) and those images in August (i.e., the month having largest fluctuations in precipitation and lake water area) in each year during 1988–2015 as examples, and the errors of lake area in different *MNDWI* threshold values during 1988–2015 were counted and demonstrated in Figure 2. The absolute percent errors in lake area from the various threshold values and our choice of threshold (0.35) were mostly within 1.5%, which indicated that the lake area was not sensitive to changes in the choice of threshold.
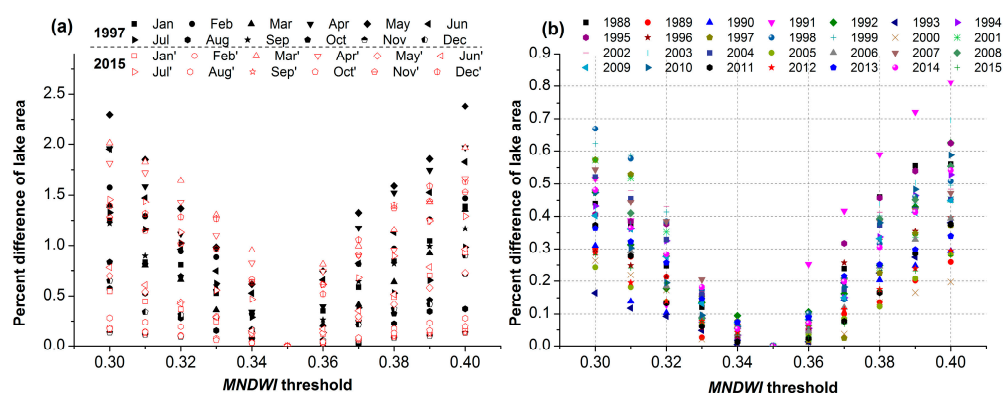
Figure 2. Examples of lake area sensitivity to the *MNDWI* (Modified Normalized Difference Water Index) threshold for the images: (**a**) in each month in 1997 and 2015; and (**b**) in August of each year during 1988–2015. The specific acquisition dates of images are shown in Table 1.

2.3.2. Remote-Sensing Identification of Lake Islands

As lake size declined, more than ten islands with remarkably different sizes were successively exposed in different locations in the lake. When lake water levels continued to decrease, some islands could connect to the mainland, thereby ceasing to be islands. The location of this connection to the mainland was the boundary between lake water and non-water features (the mainland), and this location was the source of error when using the *MNDWI* to extract lake surface area (see in Section 2.3.1). Although the absolute percent difference in lake area based on our choice of threshold was mostly within 1.5% (see in Section 2.3.1), when assuming the average absolute percent difference as 0.75% and setting the average lake area of 44.36 km^2, the area error was estimated at 0.3 km^2. The average total size of islands (0.01–0.22 km^2) was far less than the corresponding lake size (30.90–55.02 km^2), and the total island area accounting for only 0.03–0.52% of the corresponding lake area. The estimated area error (0.3 km^2) was larger than the maximum islands area. This situation makes it impossible to use the same *MNDWI* method to identify and extract these small islands.

Thus, we must use artificial visual interpretation approach to identify and extract small lake islands. The processes for this method were as follows: Step 1 was the combination of the SWIR2, SWIR1 and green bands in ENVI 5.1 for each Landsat image, which would yield a good distinction between water and land (islands). Step 2 was the loading of this combined image into ArcGIS 10.1 and the artificial identification of the status of each island to determine if it needed to be extracted or to be reclassified as not an island. Step 3 was the extraction of the boundaries and calculations of the areas of the islands in ArcGIS 10.1.

2.3.3. Field Observation and Survey of Relict Gull Populations

The field surveys of the Relict Gull population in HL were carried out by experts from the Forest Station of Shaanxi Yulin City and the Shanxi Institute of Zoology [24,25]. From April to September during 2001–2015, Xiao et al. [24,25] invested a great deal of time and energy to observe the Relict Gull population using a professional telescope (NIKON 40×) on the bank and visit all the islands to record the nests, eggs, and nestling mortality at the right time. Thus, the recorded and published data on the Relict Gull populations are scientific and convincing.

2.3.4. Estimation of Potential Evaporation in the HL Basin and Watershed Analysis of Reservoirs

As one of important climatic factors, potential evaporation (ET_0) in the HL basin was calculated due to lack of available observed data. The annual potential evaporation (ET_0) is the sum of the daily data. The daily ET_0 is calculated using the Penman–Monteith equation recommended by FAO [48]:

$$ET_0 = \frac{0.408\Delta(R_n - G) + \gamma\frac{900}{T_a+273}u_2 VPD}{\Delta + \gamma(1 + 0.34u_2)} \tag{2}$$

where Δ is the slope of the saturated vapor pressure (kPa·°C^{-1}). R_n is the net radiation at the canopy surface (MJm^{-2}·d^{-1}), and the two key coefficients (i.e., a_s and b_s) were optimized according to Liu et al. [55] to improve the estimation of ET_0. G is the soil heat flux density (MJm^{-2}·d^{-1}). γ is the psychrometric constant (kPa·°C^{-1}). T_a is the mean daily air temperature at 2-m height (°C). u_2 is the wind speed at 2-m height (ms^{-1}). VPD is the vapor-pressure deficit between saturated and actual vapor pressure (kPa).

Hydraulic engineering construction (i.e., two reservoirs) is an important human factor. Accurate controlled areas of two reservoirs were determined by watershed analysis using the software ArcSWAT2012.10.0.15 (i.e., an ArcGIS extension and graphical user input interface for Soil and Water Assessment Tool (SWAT)) (see in http://swat.tamu.edu/software/arcswat/). Watershed analysis is easily conducted using ArcSWAT. The watershed analysis processes were as follows: Step 1 was the loading of a 30-m DEM in the HL basin. Step 2 was to calculate "flow direction and accumulation". Step 3 was to "create streams and outlets", and after assigning the reservoir outlet as the final outlet,

the watershed was automatically divided. Step 4 was the calculation of the area of the divided reservoir's watershed.

2.3.5. Statistical Methods for Trend Analysis and Correlation Analysis

Three statistical methods, cumulative anomaly analysis, linear regression analysis and Pearson correlation analysis, were used to investigate the trends in the time series data and the relationships between lake area and the drivers behind changes in lake area. Cumulative anomaly analysis is a method commonly used to diagnose trends and help catch turning points in time series data [47,56–58]. Linear regression analysis was used to analyze the trends and variation rate of hydrological and meteorological variables in different periods [59]. The slope of the linear regression equation is regarded as the variation rate during the specific period [60–62]. The significance of the correlation can be determined by the size of the Pearson correlation coefficient. The linear regression analysis and Pearson correlation analysis were conducted in SPSS Version 19.0.

3. Results

3.1. Changes in the Area of Hongjian Lake

Figure 3 shows the variation in annual lake area and the lake area anomaly. During 1988–2015, the lake area presented a large fluctuation with an overall downward trend. The average, standard deviation, and change trend values of annual lake area were 44.36 km^2, 8.15 km^2, and -0.94 km^2/year, respectively. Two phases of lake variations were diagnosed by the cumulative anomaly analysis and the five-year moving average. In Sub-Period I (1988–1998), the lake area fluctuated between 50.42 km^2 and 55.02 km^2, and exhibited a weak increasing trend of 0.21 km^2/year. The average and standard deviation of lake area in Sub-Period I were 52.88 km^2 and 1.56 km^2, respectively. During Sub-Period II (1999–2015), the lake area decreased dramatically from 49.41 km^2 in 1999 to 30.90 km^2 in 2015 with a decreasing trend of -1.04 km^2/year. The lake area in 2015 decreased by 37.5% compared to that in 1999. The average and standard deviation values of lake area in Sub-Period II were 38.85 km^2 and 5.34 km^2, respectively. Compared to that during 1988–1998, the average annual lake area during 1999–2015 was decreased by 26.5%.
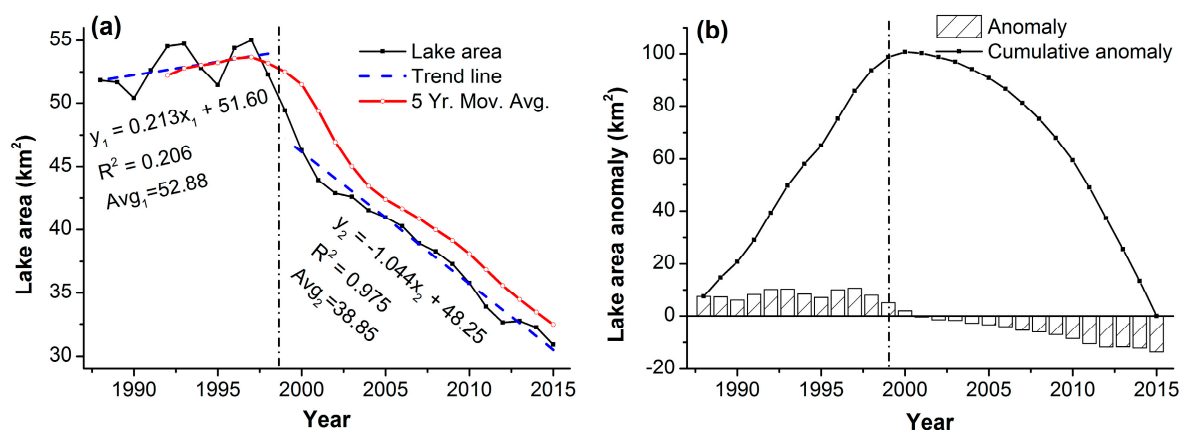
Figure 3. Variations in: (**a**) the Hongjian Lake area; and (**b**) lake area cumulative anomaly during 1988–2015. Avg stands for average, and 5 Yr. Mov. Avg. refers to the five-year moving average.

Figure 4 shows the spatial characteristics of the variations in lake area during 1988–2015, which were consistent with the results in Figure 3. HL, which has an irregular triangular shape, has exhibited rapid shrinkage since 1999, and the regions of shrinkage are mainly concentrated at the vertices and along the bottom side of the triangle, which are also the main entrances of the rivers flowing into the lake.
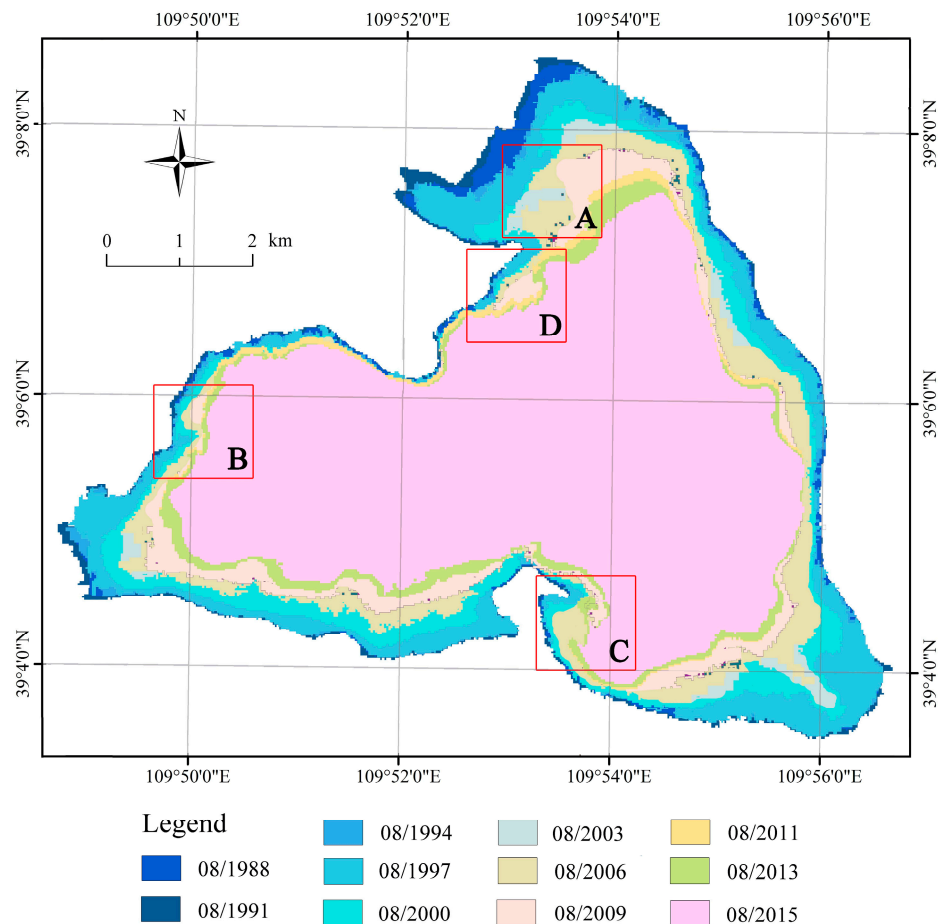
Figure 4. The spatial distribution of Hongjian Lake (HL) during 1988–2015. Four zones of lake islands are marked A, B, C, and D.

3.2. Changes of Relict Gull Habitat in Hongjian Lake

The fluctuation of lake size led to corresponding variations in island size. Differences in location, elevation and terrain resulted in the different characteristics of each island. More than ten islands that had outcropped in the form of an island group (zone) were investigated using remote sensing when the lake water level fluctuated, and each group consisted of three to five small islands. Four zones of islands, marked A, B, C, and D according to location, were successively exposed in Hongjian Lake (HL). Figure 5 shows the variations in the areas of island zones, and Table 2 provides some important information about the island zones. During 1988–2015, the island zones showed drastic fluctuations in response to the variations in lake area. The total area of the island zones ranged from 0.02 km^2 in 1998 to 0.22 km^2 in 2004. The average and standard deviation values of the island zones' area were 0.09 km^2 and 0.06 km^2. The area curve for each zone roughly showed an irregular downward parabola. As the lake area decreased steadily, the islands in each zone went through a similar process in which the islands appeared, gradually increased in area, reached a maximum area, and then the island area declined rapidly. The ranges of dates during which islands in Zones A, B, C, and D were exposed are 1988–2012, 2000–2003, 2000–2015, and 2007–2014, respectively. The areas of Zones A, B, C, and D ranged from 0–0.16 km^2, 0–0.06 km^2, 0–0.08 km^2, and 0–0.08 km^2, respectively. According to the length of for which the islands were exposed and the size of island zone, Zone A and Zone C were most likely the main locations of Relict Gull habitat, though Zone B and Zone D played a smaller roles as the habitat in some short periods. Since 2014, Zone C has been the only island zone in HL. Depending on the evolution of the island and its different states, four representative statuses for each island zone (Table 2) are selected in sequence as follows: the starting time (A1/B1/C1/D1), the time of

the largest island area (A2/B2/C2/D2), the ending time (A3/B3/C3/D3), and the nonexistence time (A4/B4/C4/D4). The spatial distribution characteristics of outcropped islands are shown in Figure 6.
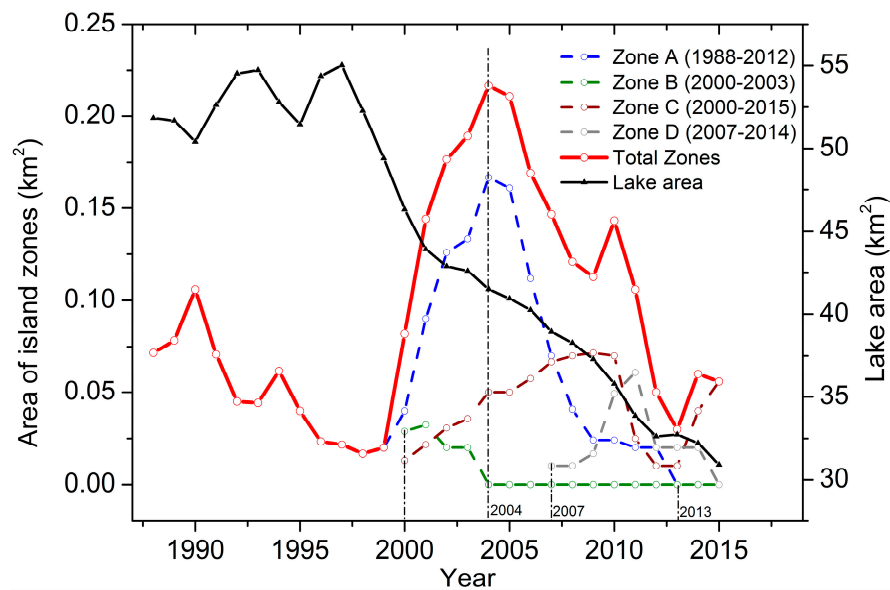
Figure 5. Variations in the area of island outcropping zones in Hongjian Lake. As lake area fluctuates, the four islands (marked A, B, C, and D) were successively exposed, and the range of time for which each zone was exposed is labeled between the brackets.

Table 2. Information about island zones and their status in Hongjian Lake during 1988–2015.

| Zones	Existence Date Span [a] (MM/YY)	Area Extent (km^2)	Status [b]	Acquisition Date (MM/YY)	Islands Area (km^2)	Lake Area (km^2)
A	January 1988–May 2012	0–0.16	A1	January 1988	0.08	51.07
			A2	June 2005	0.16	39.98
			A3	May 2012	0.02	32.96
			A4	June 2012	0	32.28
B	March 2000–July 2003	0–0.06	B1	March 2000	0.01	47.38
			B2	August 2002	0.06	43.19
			B3	July 2003	0.02	42.81
			B4	August 2003	0	42.41
C	June 2000–December 2015	0–0.08	C1	June 2000	0.01	46.76
			C2	June 2010	0.08	36.05
			C3	December 2015	0.07	30.11
			C4	May 2000	0	46.92
D	May 2007–August 2014	0–0.08	D1	May 2007	0.01	39.23
			D2	August 2011	0.08	33.67
			D3	August 2014	0.02	32.72
			D4	September 2014	0	32.64

[a] The existence date span refers to the date range for which outcropped islands were exposed during the study period (i.e., January 1988–December 2015). [b] Four representative statuses for each island zone are selected and are sorted in sequence as follows: the starting time (A1/B1/C1/D1), the time of the largest island area (A2/B2/C2/D2), the ending time (A3/B3/C3/D3), and the nonexistence time (A4/B4/C4/D4).

Relict Gull only chooses lake islands as its habitat. When the lake island areas varied, Relict Gull population quickly presented the corresponding responses. Figure 7 shows the relationships between the variations in Relict Gull populations and the variations in lake island area. The variations in the Relict Gull population can be divided into two sub-periods: the first sub-period, 2001–2010, was period of rapid population growth, and the second sub-period, 2011–2015, was period of rapid population decline. The Relict Gull population increased from 174 in 2001 to the maximum value of 15,494 in 2010,

and the population decreased from 15,412 in 2011 to 4000 in 2015. During 2001–2015, the change in the Relict Gull population was consistent with the change in total island area with the exception of a few years (i.e., 2005–2007). Compared with the four specific island zones, the Relict Gull population also remained consistent with the areas of the different zones in the different sub-periods. Specifically, the change in the Relict Gull population was consistent with changes in Zone A and Zone C during 2001–2004, with changes in Zone C during 2005–2007, and with changes in Zone C and Zone D during 2008–2015.
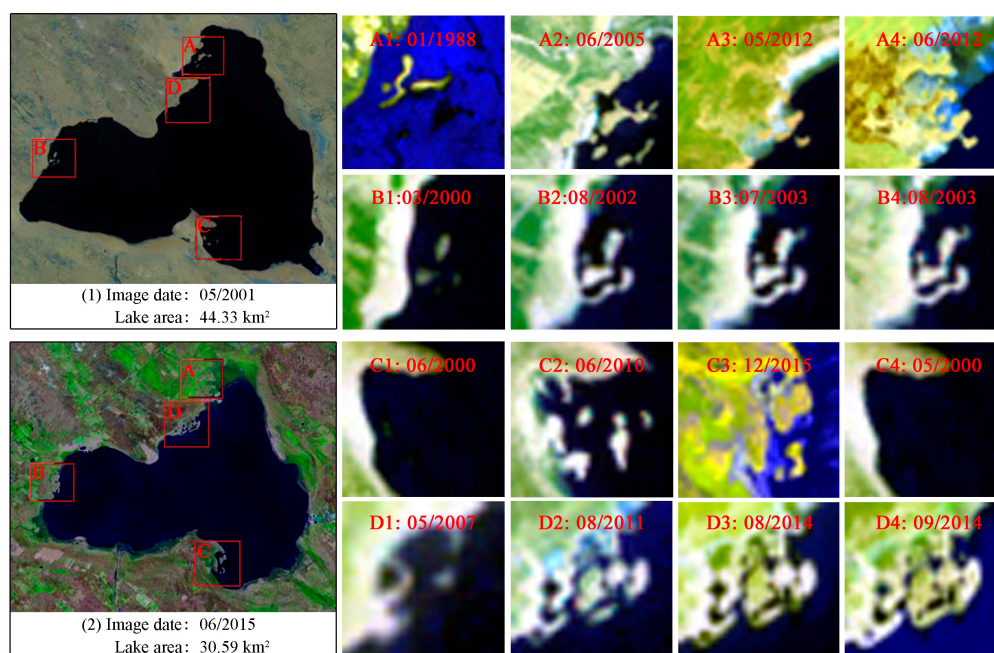
Figure 6. Examples of representative spatial distribution characteristics of outcropped islands (i.e., the four zones of islands marked A, B, C, and D) in Hongjian Lake on different dates. Locations of the four zones are labeled in the left base maps (i.e., (1) and (2)).
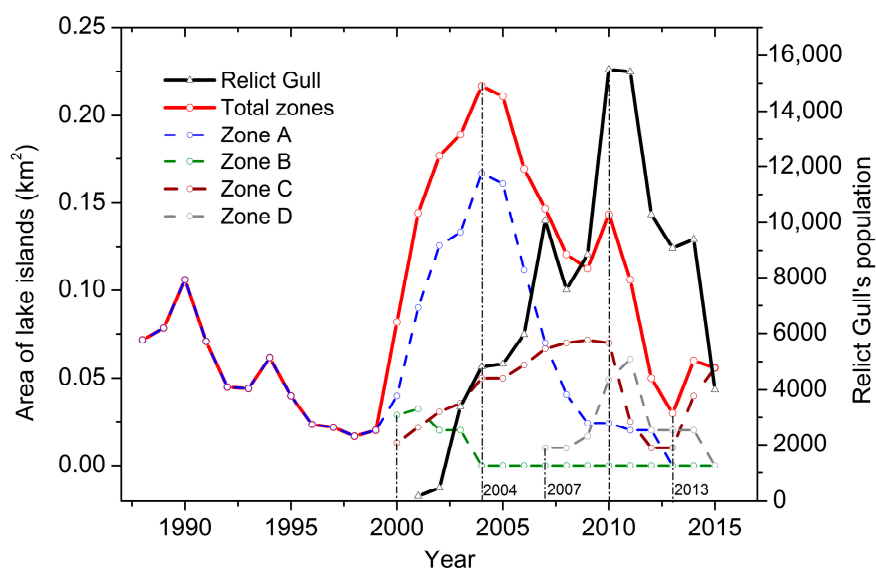

Figure 7. Relationships between the variations in Relict Gull population and the variations in the areas of the lake islands (including the total area of islands and the area of the four zones marked A, B, C, and D).

3.3. Changes in Climatic Factors and Human Factors

Here, ten driving factors affecting the lake area were analyzed, including the three representative climatic factors (i.e., precipitation (*P*), temperature (*T*), and potential evapotranpiration (ET_0)) and the seven indictors of human activity (i.e., area of land use types, Normalized Differential Vegetation Index (*NDVI*), human population (*HP*), sheep population (*SP*), gross industrial output value (*GIOV*), hydraulic engineering construction, and tourism development). It is worth noting that the turning points of these factors were not completely the same as that in the lake area; however, to better reveal the synchronous reasons for variations in the lake area, the sub-periods of these factors were unified as the same two sub-periods corresponding to lake area, including Sub-Period I (1988–1998) and Sub-Period II (1999–2015).

Variations in the three representative climatic factors, namely annual precipitation (*P*), temperature (*T*), and potential evapotranspiration (ET_0), are shown in Figure 8. *P* exhibited a drastic fluctuation with the range of 214.7–576.5 mm during 1988–2015. The average and standard deviation of *P* were 380.7 mm and 81.9 mm, respectively. In Sub-Period I (1988–1998), the average, standard deviation, and change trend values of *P* were 390.8, 66.2, and −1.1 mm/year, respectively. However, in Sub-Period II (1999–2015), the average, standard deviation, and change trend values of *P* became 374.1, 92.0, and 7.7 mm/year, respectively. The average annual *P* in 1999–2015 decreased 16.6 mm, accounting for −4.3% of that in 1988–1998. In addition, more larger fluctuations and more extreme events occurred in 1999–2015. For example, extreme dry years appeared in 1999, 2000, 2005, and 2006, with *P* values of 262.1 mm, 214.7 mm, 257.3 mm, and 298.5 mm, respectively. The years 2012 and 2013 experienced extreme heavy rain, with *P* values of 479.2 mm and 576.5 mm, respectively. The fluctuation in annual *T* during 1988–2015 is shown in Figure 8b. The temperature ranged from 6.3 °C in 1988 to 8.8 °C in 2015, with an average and standard deviation of 7.6 °C and 0.7 °C, respectively. In Sub-Period I, the range, average and standard deviation of *T* were 6.3–7.8 °C, 7.2 °C, and 0.11 °C, respectively. In Sub-Period II, the range, average and standard deviation of *T* became 7.2–8.8 °C, 8.0 °C, and 0.03 °C, respectively. The average annual *T* during 1999–2015 increased to 0.8 °C, representing an 11.4% increase relative to that during 1988–1998. Similarly, Figure 8c shows the variations in annual ET_0, which has a range of 929.6–1117.1 mm. During 1988–1998, the average and standard deviation of ET_0 were 1027.4 mm and 33.3 mm, respectively. During 1999–2015, the average and standard deviation of ET_0 were 1050.5 mm and 50.7 mm, respectively. Compared with that during 1988–1998, the average annual ET_0 during 1999–2015 increased by 23.2 mm, representing an increase of 2.3%. Therefore, the climate condition in the HL basin became more drier, warmer, and fluctuant, which was expressed by the decrease of average annual *P*, the increase of average annual *T* and ET_0, and the arising of more extreme events.
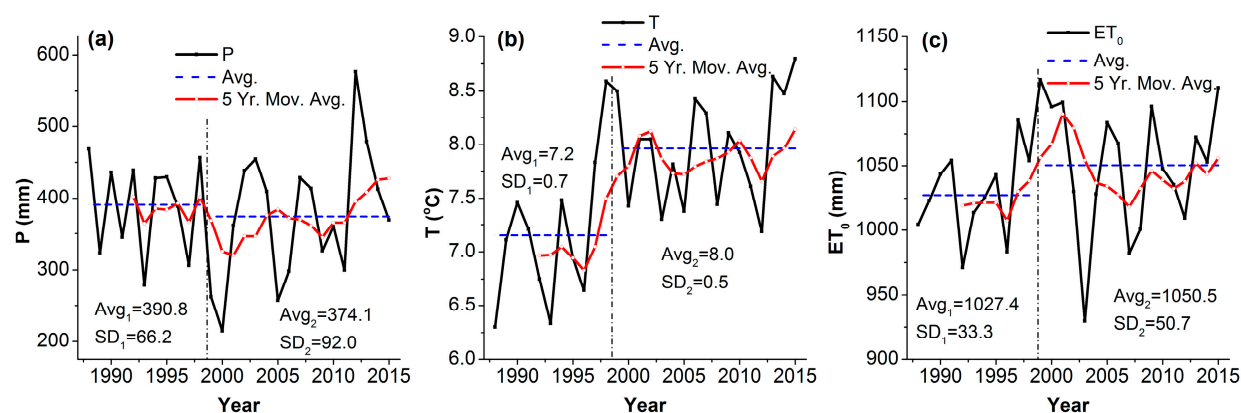
Figure 8. Variations in three climatic factors: (**a**) annual precipitation (*P*); (**b**) annual temperature (*T*); and (**c**) annual potential evapotranspiration (ET_0).

The variations in the seven indictors of human activity during 1988–2015 are shown in Figures 9 and 10. Figure 9a,b shows the variations in the main underlying surface of HL basin expressed by the area of the land use types and the *NDVI*, which were used as alternative indicators of irrigation water usage and vegetation water consumption. The average areas of farmland, woodland, and grassland during 1988–2015 were 231 km^2, 86 km^2, and 686 km^2, respectively, accounting for 17.1%, 6.3% and 50.7% of the total HL basin. The total area of farmland, woodland, and grassland increased from 995 km^2 in Sub-Period I (1988–1998) to 1007 km^2 in Sub-Period II (1999–2015), representing an increase of 1.2%. Though the area of farmland declined by 39 km^2, the total area of woodland and grassland inclined by 51 km^2. Moreover, the *NDVI* values in the HL basin during 1988–2015 had increasing trends. The average annual *NDVI* values in 1988–1998 and 1999–2015 were 0.18 and 0.22, respectively, representing an increase of 19.5%. Figure 9c,d shows human population (*HP*), sheep population (*SP*), and gross industrial output value (*GIOV*) of the four towns (i.e., Xinjie Town, Taigesumu Town, Zhongji Town, and Erlintu Town) in the HL basin. These three factors showed increasing trends during 1988–2015. During the sub-period of 1988–1998, these factors had relatively low values with slow increasing trends, which indicated that the domestic water and industrial water usage in the basin were low. After 1999, except for the slight decrease in the human population during 1999–2003, these factors maintained fast increasing trends with higher values, which indicated that the corresponding domestic water and industrial water usage were increasing as well.
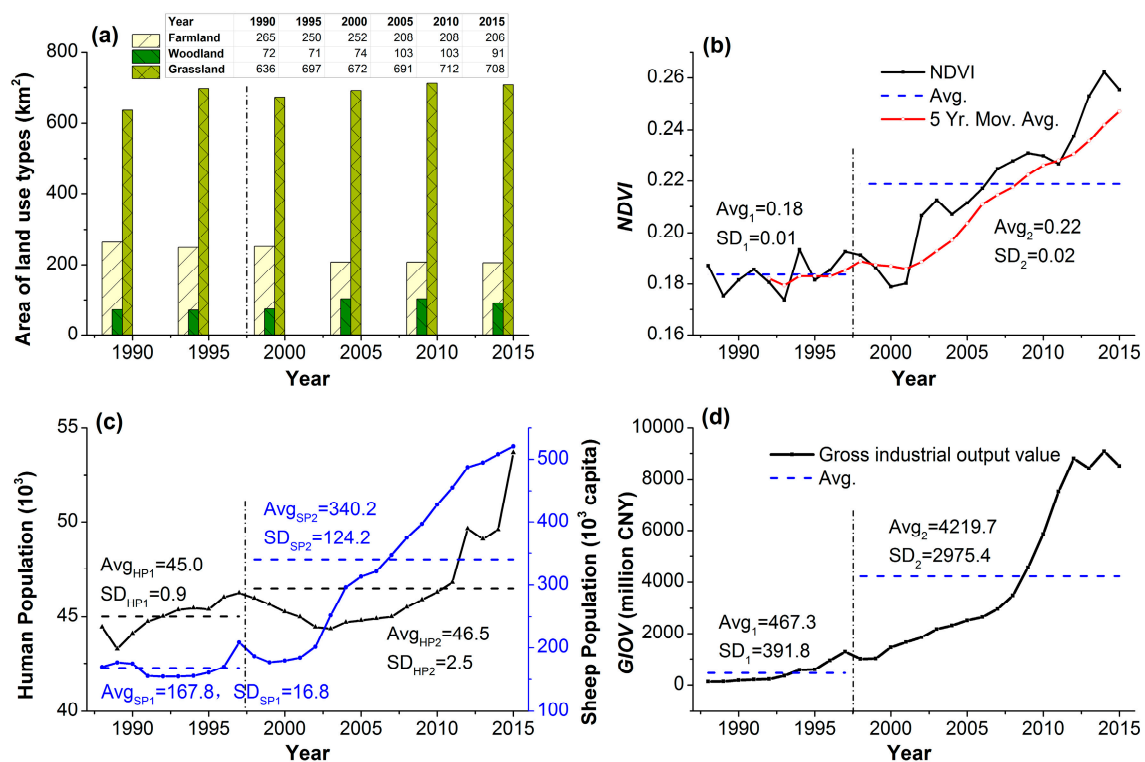
Figure 9. Variations in: (**a**) area of land use types; (**b**) *NDVI* value; (**c**) Human population and sheep population; and (**d**) Gross industrial output value of the four towns (i.e., Xinjie Town, Taigesumu Town, Zhongji Town, and Erlintu Town) during 1988–2015 in the HL basin.

In addition, hydraulic engineering construction and tourism development around HL were another two important human factors. Figure 10a,b shows the two main reservoirs and their surrounding environments in the HL basin. The Zhashake Reservoir and the Maogaitu Reservoir, which are located in the Zhashake River and the Maogaitu River (Figure 1), appeared in 2005 and 2009, respectively. The results of the watershed analysis revealed that the watershed areas controlled by the Zhashake Reservoir and the Maogaitu Reservoir were 227 km^2 and 284 km^2, respectively, accounting

for 16.8% and 21.0% of the total basin area (i.e., 1352 km^2). In total, 37.8% of the total basin area was intercepted by the two reservoirs, cutting off the original inflow into HL. Particularly notable was that the Zhashake River and the Maogaitu River are located in the Inner Mongolia Autonomous Region, and are managed by the Water Conservancy Bureau of the Inner Mongolia Autonomous Region, while HL is administered by The People's Government of Shaanxi Province. This situation mixed cross-administrative districts can easily to lead to conflicts for water resources, especially in these dry regions. The two most important water-supply tributaries of HL were intercepted, which was bound to have a clear influence on the area of the lake. Regarding to the development of tourism around HL, especially the construction of amusement parks and docks around the lake (e.g., the Daolaoyaoze amusement parks located in the northwest of HL and the tour service area and docks located in the eastern region of HL, see in Figure 10c,d) was another impact factor. HL was officially recognized as a provincial scenic spot in 1995, and was upgraded to a national 4A-level scenic spot in 2012. During 1999–2006, 2007–2011, and 2012–2015, the average annual number of visitors reached 133,000, 200,000, and 250,000, respectively, and these values were approximately three, four, and five times greater than the local average annual human population in the same sub-period. The fast growth of tourism, to a large extent, resulted in the increase of local water consumption.

Figure 10. (**a**) The Zhanshake Reservoir; (**b**) the Maogaitu Reservoir in the HL basin; (**c**) the Daolaoyaoze amusement parks located in the northwest of Hongjian Lake; and (**d**) the comprehensive tour service area and docks located in the east of Hongjian Lake. The date of the SPOT-5 images is 6 August 2015, and the images have a 2.5 m-resolution.

3.4. Correlation Between the Lake Area and Its Driving Factors

The corresponding change process of the area of HL and the driving factors behind the changes is plotted in Figure 11, and the correlation coefficients are shown in Table 3. Because of different units and magnitude of variables, to better illustrate the detailed change process of lake area and its driving factors in the same diagram, we normalize the lake area and the driving factors to 0–1. During 1988–2015 and the two sub-periods (1988–1998 and 1999–2015), although all the variables had a drastic variation, the different degrees of correlation between the lake area and the driving factors still could be visually observed (Figure 11), and the correlation coefficients had obvious differences (Table 3).

Specifically, in Sub-Period I (1988–1998), the human factors (i.e., *NDVI*, *HP*, *SP*, and *GIOV*) had a small magnitude, which meant that the human activity was low. Thus, Sub-Period I could be regarded as the "natural period", and the lake area showed natural up and down fluctuations as climatic factors fluctuated (i.e., *P*, *T*, and ET_0). The correlation coefficients between the lake area and the three climatic factors were larger than that with the human factors. In Sub-Period II (1999–2015), especially after 2002, the human factors became more intensive with a larger magnitude and strong linear increasing trends, and the lake area in this sub-period was more disturbed by human factors. Although the climatic factors in Sub-Period II still fluctuated up and down, the corresponding lake area only decreased dramatically. The correlation coefficients between the lake area and the human factors became larger and more significant ($p < 0.01$) than that with the climatic factors. It is worth noting that the coefficients with climatic factors in 1999–2015 decreased distinctly in comparison to that in 1988–1998. The higher and significant negative correlation coefficients with human factors in Sub-Period II could indicate that the human activity had more important effects on the variations in the area of HL.

Table 3. The Pearson correlation coefficient between the area of HL and its driving factors.

	P	*T*	ET_0	*NDVI*	*HP* [1]	*SP* [2]	*GIOV* [3]
HL area 1988–2015	−0.15	−0.56 **	−0.18	−0.92 **	−0.61 **	−0.94 **	−0.91 **
HL area 1988–1998	−0.50	−0.18	−0.22	−0.02	0.62 *	0.06	0.46
HL area 1999–2015	−0.48	−0.19	0.10	−0.94 **	−0.76 **	−0.98 **	−0.94 **

[1] *HP* stands for human population, [2] *SP* means sheep population, and [3] *GIOV* stands for gross industrial output value. The significance level is indicated by * and **, representing $p < 0.05$ and $p < 0.01$, respectively.
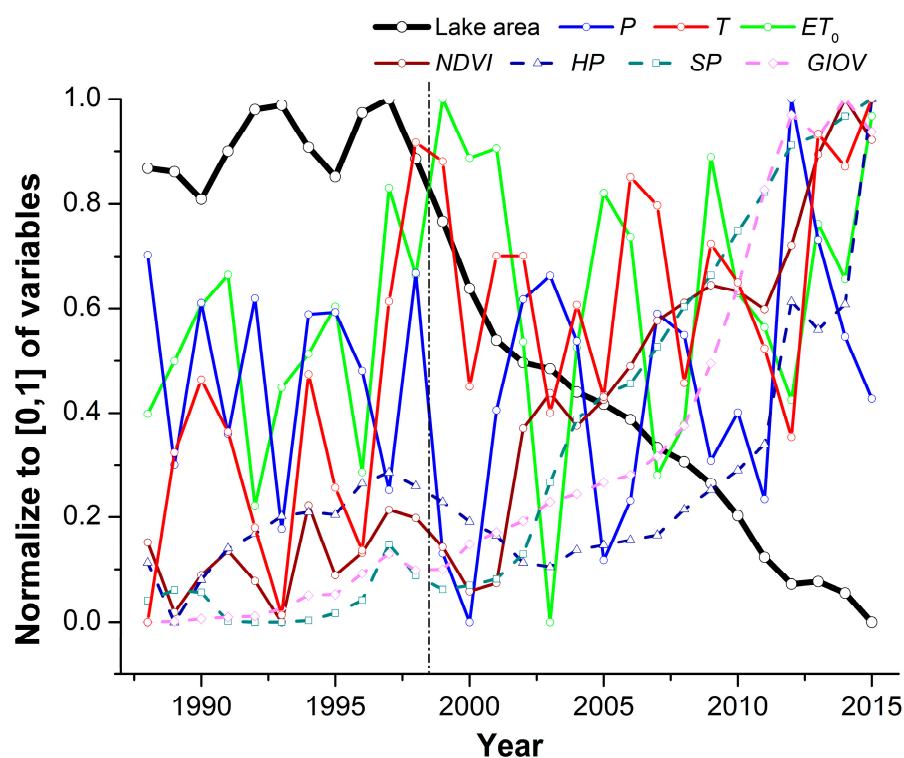
Figure 11. Comparison of normalized lake area and the normalized driving factors (normalized to 0–1).

Thus, in Sub-Period I (1988–1998), the relatively high level of *P*, the low evapotranspiration (expressed by low *T* and low ET_0), as well as the low level of human activity caused the weak increase in the area of HL. However, in the second period, 1998–2015, the climate became warmer (expressed by lower *P*, higher *T* and ET_0), which meant a decrease in the natural recharge of the lake and an increase in natural water consumption. Simultaneously, the human activity became stronger, indicated by the

increase in grassland and woodland, the higher *NDVI* values, the faster increase in human population, the higher sheep population and gross industrial output value, the direct inflow interception by the two reservoirs, and the more rapid development of tourism, which resulted in greater water consumption for human activity. The more severe human activity as well as climate warming caused a fast decrease in the area of HL in Sub-Period II (1999–2015).

4. Discussion

4.1. Variations in Lake Size, Lake Island Area and the Driving Factors

The remote-sensing investigation of variations in lake size and lake island area and the analysis of the driving factors behind these variables are our most important research target, and each was analyzed in Section 3. More detailed change characteristics and a comparison with other research are discussed here.

First, regarding the temporal variations in lake area, others research [37,39–43] and the results of our study revealed that the water surface area of HL had an overall downward trend and suffered from severe shrinkage. However, the specific area and its change processes exhibited some differences due to different remote sensing data sources, the amount of data, the methods for extracting the lake surface area, and the study period. Comparison of lake area in other research and in our study is shown in Figure 12. Specifically, Zhao et al. [37] used only eight images from Landsat MSS, TM, ETM+ and OLI during 1973–2013 to extract the lake area using the *NDVI* and human-computer interactive interpretation. Liu et al. [43] constructed a scaled Soil Moisture Monitoring Index (S-SMMI) on the basis of 21 images during 1988–2014 from Landsat TM, ETM+ and OLI to extract the lake area. Wang et al. [41] used 25 images from Landsat MSS, TM, and ETM+ during 1973–2009 to extract the lake area based on the mixed pixel decomposition. Li et al. [40] used only three images from Landsat TM to extract the lake area during 1986–2007. Liu et al. [42] used the MODIS vegetation index product during 2000–2014 to extract the lake area based on Soil Moisture Monitoring Index (SMMI). Yin et al. [39] used the MODIS vegetation indices products during 2000–2007 to extract the lake area by artificial visual interpretation. Compared to that in our study, the range of relative error of the average lake area in the above research was −3.3%–4.5%, −4.1%–3.9%, −4.1%–5.4%, 0.9%–3.6%, −1.7%–8.6%, and −3.2%–10.6%, respectively. In addition, in terms of the specific change processes, except for that in Liu et al. [43] and the results of our study, the sub-period of increasing trend during 1988–1998 was not clearly indicated in other research. This situation could show that the specific lake area and its processes as shown in Landsat imagery were generally more similar with those in our study than those shown in MODIS imagery. In addition, the change process was captured and demonstrated with more detail and accuracy when using a greater number of images with more detail and at higher-resolutions.

Second, regarding the spatial variation characteristics of HL, compared with the previous research [37,40–43], even though the specific periods of interest were not the same, the spatial characteristics of shrinkage and the regions where shrinkage was mainly concentrated, the three vertices and the bottom side of the triangle (lake), were very similar. HL is in a closed basin, and the topography of the lake basin is the lowest in the middle and is higher on the outside. When the lake water level declines, the outside regions are the first to be exposed. For the outside regions at different locations, the extent of shrinkage (or occasionally, extension) in the horizontal direction exhibited significant differences. The outside regions with flatter and more shallow terrain (e.g., the three vertices of lake) had a larger extent of shrinkage and more sparse contour lines than steep and deep regions (e.g., the middle regions of the left and right sides of the triangle in Figure 4). In addition, the regions at the three vertices of lake were also the main inflows of the rivers flowing into the lake (see Figures 1 and 4), which made these regions to be the first affected when a sharp drop in inflow occurred.
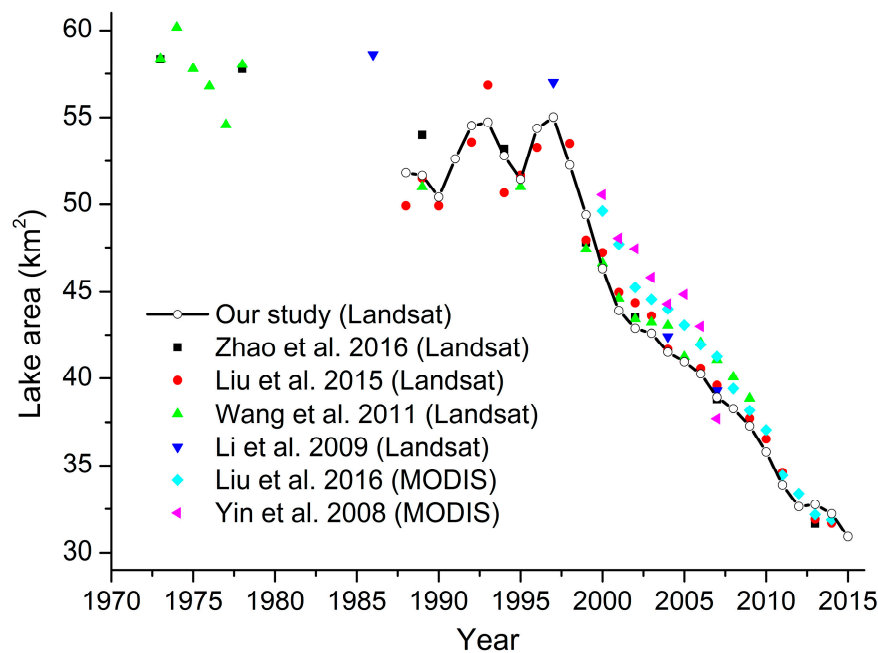
Figure 12. Comparison of the lake surface area in our study and other studies.

Third, regarding the variations in lake islands (i.e., Relict Gull habitat) in HL, though the importance of lake islands to Relict Gull reproduction has been gradually recognized, only a few studies have been conducted since Relict Gull was first found in HL in September 2000 [24,25]. Xiao et al. [24,25] conducted a field survey of the main lake islands during 2001–2008 and found that two main groups of islands existed, one in the northwest and another in the southern region of HL. In addition, both groups of islands did have Relict Gull nests and individuals. The estimated area of each group of islands in June 2008 was approximately 0.04 km^2. This finding was similar to that in our study, but a more long-term dynamic change process for the islands was revealed in our study in detail. In fact, we found that Zone A and Zone C were the main lake islands in HL during 2001–2008 and that the two groups of islands in the northwest and in the southern region were the islands in Zone A and Zone C in our study (see Figure 6), with areas of 0.04 km^2 and 0.07 km^2 at the same time, respectively. In addition, we found that another two groups of islands, namely Zone B and Zone D, existed in 2000–2003 and in 2007–2014, respectively. Zone B and Zone D were likely to have Relict Gull nests and individuals. In our study, the high correlation between the Relict Gull population and the areas of lake islands, especially those of island Zone A and Zone C, could support the following two facts. First, our findings verified that Relict Gull only takes island in lakes as breeding habitat [20–22]. Second, our findings verified that island Zone A and Zone C (called Hongshi island by the local people [27]), were the most important breeding habitats for Relict Gull in the HL basin. Moreover, the form of several groups of islands (i.e., not one single island or not only one single group) should have attracted sufficient attention. Rather than forming a single lake island in Bojiang Lake [23], HL easily forms outcrops of more small islands, meaning more space for Relict Gull habitat due to the relatively great water depth and water area of HL. As the size of HL declined, the islands outcropped in the form of the four island zones (i.e., Zone A, B, C, and D), and each zone consisted of several small islands. The formation of island zones steadily provided enough space for Relict Gull breeding grounds, thereby counterbalancing the damage due to the continuous shrinkage of the lake. Existence of lake islands is an essential condition for Relict Gull breeding. Unfortunately, there has been only one group of islands (i.e., Zone C) in HL since 2014 (see in Figure 5 and Table 2). If the lake water level continues to drop in the near future, whether Zone C will continue to exist is unclear, and whether new islands will emerge is also unknown. Therefore, it is very important and necessary to carry out topographic and bathymetric surveys of the lake.

Lastly, regarding the driving factors affecting variations in the lake area, both other research [34–36,39,40,42] and our study revealed that the reasons for shrinkage of HL were climate change and human activity. Precipitation and temperature (or evapotranspiration) were generally chosen as the climatic factors and have been thoroughly quantitatively analyzed. These analyses were similar to that in our study. However, due to a lack of statistical data and the difficulty of the data acquisition and calculations, some human factors are nearly impossible to quantitatively demonstrate and analyze, such as direct water abstraction (for irrigation, industry, and domestic uses), direct water interception by reservoirs, and indirect water consumption by vegetation. These human factors have been addressed more frequently through qualitative analysis. In our study, we attempted to choose some available quantitative indicators (e.g., area of farmland, woodland and grassland; *NDVI*; human population; sheep population; gross industrial output value; watershed area controlled by the reservoirs; and average annual visitors) as indirect proxies for direct water use and consumption. Though the corresponding change process and correlation were clearly shown, the further accurate statistics of the direct water use is very important and necessary for analysis to variation mechanism of the lake area and the water resources management in the HL basin. Moreover, though the two sub-periods were uniformly divided at 1999 in our study, the turning points for some climate factors and human factors were not completely the same as that of the lake area (in 1999), including the turning points for T, ET_0, and *NDVI* in 1997, 1990 and 2001, respectively. These different turning points could reflect the complexity of variations in lake area to some extent and could suggest that the lake area change was not decided by a single factor. Another notable was that extreme precipitation occurred more frequently in Sub-Period II (1999–2015). In the context of more intensive human activity, extreme lower precipitation in some years, such as 1999–2000 and 2005–2006, was bad for the lake area recovery. Even though extreme heavy precipitation happened in 2012 and 2013, the lake shrinkage was still not effectively alleviated, and the lake area seemed no recovery.

4.2. Implications to the Protection for Lake Water Resources and Relict Gull Habitat

The present study could have several implications for the protection of the water resources and Relict Gull habitat in HL. First, a long-term monitoring for the lake area and lake islands is necessary for further hydrological and ecological studies. The remote-sensing monitoring using Landsat imagery is an effective method, and the regular in site field measurement is also needed. Second, compared with the highly random climatic factors, the more subjective and controllable human activity has become the main driving forces behind variations in lake area; thus, human activity requires more attention, should be more restrained. It is both thought-provoking and discouraging that the rapid development of the local economy and social development have taken place at the expense of the environment. Third, the direct human water use (i.e., domestic water, livestock water, irrigation water, and industrial water) require more detailed monitoring. The green water consumption by vegetation (crops, woodland, and grassland) requires accurate calculation. Monitoring of direct human water use and estimation of vegetation water consumption can be useful for the accurate assessment to water resources in the HL basin and the net inflow to the lake. Fourth, the current situation of only some islands in Zone C existing is not good news to Relict Gull's survival and breeding. Taking accurate topographic mapping of lake is necessary for confirming whether new islands will emerge if the lake water level continues to drop in the near future. Simultaneously, the artificial excavation and modification to make some land-tied islands (previous the lake islands) reborn as lake islands may be an effective way to keep essential habitat for Relict Gull. Especially, if no any new islands will emerge as the lake water level continues to drop in the near future, excavation and modification of islands to provide enough essential living space for Relict Gull breeding should be paid enough attention by the local administrations. The early testing and verification in actual effects of excavation and modification of islands on Relict Gull breeding should be encouraged and studied. Existence of lake islands is essential for Relict Gull breeding. If insufficient lake islands stably exist in the near future, the Relict Gull population will be severely affected and Relict Gull will most likely abandon this important habitat. Lastly, the allocation

of water resources between the Inner Mongolia Autonomous Region and Shaanxi Province needs to be effectively addressed [39]. The two most important rivers flowing into Hongjian Lake are intercepted by the reservoirs (located in the Inner Mongolia autonomous region). This situation of cross-administrative district is easy to lead to conflicts for water resources.

4.3. Uncertainties and Limitations

Several uncertainties and limitations exist in this study. First, to ensure the continuity of the monthly remote sensing lake area data, the study period was truncated to 1988–2015, not including the 1970s and 1980–1987. In fact, some partial remote sensing data were available for HL prior to 1988 [37,41], but these data were not used in this study to avoid the uncertainty of subjective interpolation. Second, the average lake area for each month was estimated using one available remote sensing image for each month, which may result in some deviation from the actual lake water conditions. Third, the variations in island area were determined using remote sensing data with a resolution of 30 m × 30 m. Some small islands with an area below the smallest grid resolution in each of the island zones were not well identified or extracted. This approximation could have led to some deviation from the actual island area. More high-resolution remote sensing imagery is needed to address this issue in future studies. Fourth, the seven indicators of human activity were indirect proxies for direct water use (i.e., domestic water, livestock water, industrial water, irrigation water and vegetation water consumption) because accurate statistics on and the calculation of direct water use were extremely difficult to acquire and time-consuming, respectively. Lastly, the changes in lake area are only the external manifestation of the water balance in the HL basin. The variations in the water balance are the most essential reasons for variations in lake and island area. However, due to a lack of in situ hydrological monitoring data and accurate statistics on direct water use, it is extremely difficult to accurately calculate the water balance in the HL basin. Some useful hydrological prediction methods for ungauged basins [47,63,64] are recommended for future studies.

5. Conclusions

In this study, the variations in the area of Hongjian Lake (HL) and lake island area during 1988–2015 were investigated using Landsat imagery, and the driving forces behind these changes were analyzed using remote sensing data and local socio-economic data. The main conclusions were drawn as follows: (1) The lake area during 1988–2015 ranged from 55.02 km^2 to 30.90 km^2 and exhibited a large fluctuation with an overall downward trend of -0.94 km^2/year. The cumulative anomaly analysis diagnosed the lake variations as having two sub-periods with different characteristics and leading driving factors. The average and trend were 52.88 and 0.21 km^2/year during 1988–1998 and 38.85 and -1.04 km^2/year during 1999–2015, respectively. During 1988–1998, the relatively high precipitation, low evapotranspiration, and low levels of human activity resulted in a weak increase in the area of HL. However, in 1999–2015, the more severe human activity as well as climate warming resulted in a fast decrease in the area of HL. (2) The variations in lake island area were dependent on the area of HL and ranged from 0.02 km^2 to 0.22 km^2. As the lake size declined, the islands outcropped in the form of the four island zones (i.e., Zone A, B, C, and D), and each zone consisted of several small islands. The formation of island zones (i.e., multiple islands) steadily provided enough space for Relict Gull breeding grounds, counteracting the damage due to the continuous shrinkage of the lake. (3) The high correlation between the Relict Gull population and the area of the lake islands, especially island Zones A and C, verified the fact that Relict Gull only takes islands in the lake as breeding habitat. These correlations also revealed that island Zone A and Zone C were the most important breeding habitats for Relict Gull in the HL basin. (4) Human activity became the main factor for the shrinkage in the area of HL after 1999. To better protect the water resources of the lake and the habitat of Relict Gull, the more controllable human activity should receive more attention, human activity should be more controlled, there should be more detailed monitoring, and further accurate assessment should be conducted.

Author Contributions: Kang Liang conceived and designed the study, drew the figures, and wrote the paper. Guozhen Yan performed the data processing and drew the figures and tables.

Conflicts of Interest: The authors declare no conflict of interest.

References

1. Liu, H.; Yin, Y.; Piao, S.; Zhao, F.; Engels, M.; Ciais, P. Disappearing lakes in semiarid northern china: Drivers and environmental impact. *Environ. Sci. Technol.* **2013**, *47*, 12107–12114. [CrossRef] [PubMed]

2. Tao, S.; Fang, J.; Zhao, X.; Zhao, S.; Shen, H.; Hu, H.; Tang, Z.; Wang, Z.; Guo, Q. Rapid loss of lakes on the mongolian plateau. *Proc. Natl. Acad. Sci. USA* **2015**, *112*, 2281–2286. [CrossRef] [PubMed]

3. Talbot, M.R.; Delibrias, G. Holocene variations in the level of lake bosumtwi, Ghana. *Nature* **1977**, *268*, 722–724. [CrossRef]

4. Macdonald, G.M.; Edwards, T.W.D.; Moser, K.A.; Pienitz, R.; Smol, J.P. Rapid response of treeline vegetation and lakes to past climate warming. *Nature* **1993**, *361*, 243–246. [CrossRef]

5. Williamson, C.E.; Saros, J.E.; Vincent, W.F.; Smold, J.P. Lakes and reservoirs as sentinels, integrators, and regulators of climate change. *Limnol. Oceanogr.* **2009**, *54*, 2273–2282. [CrossRef]

6. Song, C.; Huang, B.; Richards, K.; Ke, L.; Hien Phan, V. Accelerated lake expansion on the tibetan plateau in the 2000s: Induced by glacial melting or other processes? *Water Resour. Res.* **2014**, *50*, 3170–3186. [CrossRef]

7. Pekel, J.-F.; Cottam, A.; Gorelick, N.; Belward, A.S. High-resolution mapping of global surface water and its long-term changes. *Nature* **2016**, *540*, 418–422. [CrossRef] [PubMed]

8. Yuan, Y.; Zeng, G.; Liang, J.; Huang, L.; Hua, S.; Li, F.; Zhu, Y.; Wu, H.; Liu, J.; He, X. Variation of water level in dongting lake over a 50-year period: Implications for the impacts of anthropogenic and climatic factors. *J. Hydrol.* **2015**, *525*, 450–456. [CrossRef]

9. Coe, M.T.; Foley, J.A. Human and natural impacts on the water resources of the lake chad basin. *J. Geophys. Res. Atmos.* **2001**, *106*, 3349–3356. [CrossRef]

10. Assel, R.A.; Quinn, F.H.; Sellinger, C.E. Hydroclimatic factors of the recent record drop in laurentian great lakes water levels. *Bull. Am. Meteorol. Soc.* **2004**, *85*, 1143–1151. [CrossRef]

11. Sellinger, C.E.; Stow, C.A.; Lamon, E.C.; Qian, S.S. Recent water level declines in the lake michigan-huron system. *Environ. Sci. Technol.* **2008**, *42*, 367–373. [CrossRef] [PubMed]

12. Ma, R.; Duan, H.; Hu, C.; Feng, X.; Li, A.; Ju, W.; Jiang, J.; Yang, G. A half-century of changes in china's lakes: Global warming or human influence? *Geophys. Res. Lett.* **2010**, *37*, L24106. [CrossRef]

13. Yang, X.; Lu, X. Drastic change in China's lakes and reservoirs over the past decades. *Sci. Rep.* **2014**, *4*, 6041. [CrossRef] [PubMed]

14. Birkett, C.M. The contribution of topex/poseidon to the global monitoring of climatically sensitive lakes. *J. Geophys. Res. Atmos.* **1995**, *100*, 25179–25204. [CrossRef]

15. Alsdorf, D.E.; Rodriguez, E.; Lettenmaier, D.P. Measuring surface water from space. *Rev. Geophys.* **2007**, *45*, RG2002. [CrossRef]

16. Song, C.; Huang, B.; Ke, L. Modeling and analysis of lake water storage changes on the tibetan plateau using multi-mission satellite data. *Remote Sens. Environ.* **2013**, *135*, 25–35. [CrossRef]

17. Mueller, N.; Lewis, A.; Roberts, D.; Ring, S.; Melrose, R.; Sixsmith, J.; Lymburner, L.; Mcintyre, A.; Tan, P.; Curnow, S. Water observations from space: Mapping surface water from 25 years of landsat imagery across australia. *Remote Sens. Environ.* **2015**, *174*, 341–352. [CrossRef]

18. Halabisky, M.; Moskal, L.M.; Gillespie, A.; Hannam, M. Reconstructing semi-arid wetland surface water dynamics through spectral mixture analysis of a time series of landsat satellite images (1984–2011). *Remote Sens. Environ.* **2016**, *177*, 171–183. [CrossRef]

19. Zhu, W.; Jia, S.; Lv, A. Monitoring the fluctuation of lake qinghai using multi-source remote sensing data. *Remote Sens.* **2014**, *6*, 10457–10482. [CrossRef]

20.　BirdLife International. *Larus relictus*. (amended version published in 2016) The IUCN Red List of Threatened Species 2017: e.T22694447A112120559. Available online: http://dx.doi.org/10.2305/IUCN.UK.2017-1.RLTS.T22694447A112120559.en (accessed on 30 September 2017).

21.　He, F.; Melville, D.; Xing, X.; Ren, Y. A review on studies of the relict gull larus relictus. *Chin. J. Zool.* **2002**, *37*, 65–70.

22.　Zhang, Y.; He, F. A study of the breeding ecology of the relict gull larus relictus at ordos, Inner Mongolia, China. *Forktail* **1993**, *8*, 125–132.

23.　Yan, G.; Lou, H.; Liang, K.; Zhang, Z. Dynamics and driving forces of bojiang lake area in erdos larus relictus national nature reserve, china. *Quat. Int.* **2017**. [CrossRef]

24.　Xiao, H.; Zhang, Z.; Wang, Z.; Wang, Y. Breding population dynamic of relict gull (*Larus relietus*) at Hongjiannao lake of Shaanxi Province. *J. Shaanxi Norm. Univ.* **2006**, *34*, 83–86. (In Chinese)

25.　Xiao, H.; Wang, Z.; Hu, C.; Wang, Y. Relict gull *Larus relictus* breeding population dynamics and their breeding habitat in Hongjian nur, Shaanxi Province. *Sci. Technol. Rev.* **2008**, *26*, 54–57. (In Chinese)

26.　Zhou, L.; Feng, N.; Zhang, B.; Wang, Z.; Lu, Z. Population dynamics and distribution of *Larus relictus* and waterfowls in Hongjiannao wetland. *Chin. J. Wildl.* **2008**, *29*, 299–301. (In Chinese)

27.　Wang, Q.; Yang, C.; Liu, Z.; Hu, C.; Xiao, H. Brooding behavior and nestling growth of relict gull in hongjiannao, shaanxi province. *Chin. J. Zool.* **2013**, *48*, 357–362. (In Chinese)

28.　Shen, J.; Wang, Y.; Xiangdong, Y.; Enlou, Z.; Yang, B.; Junfeng, J. Paleosandstorm characteristics and lake evolution history deduced from investigation on lacustrine sediments—The case of Hongjiannao lake, Shaanxi Province. *Chin. Sci. Bull.* **2005**, *50*, 2355–2361.

29.　Fang, T.; Xu, Q.H.; Li, Y.C.; Cao, X.Y.; Wang, X.L.; Zhang, L.Y. Pollen assemblage characteristics of lakes in the monsoon fringe area of china. *Sci. Bull.* **2008**, *53*, 3354–3363.

30.　Li, S.; Chen, S.; Zhang, J. Environmental changes analysis of hongjiannao lake during recent fifty years—Based on the data of lake sediments. *Agric. Sci. Technol.* **2009**, 178–183.

31.　Li, D.; He, H.; Liu, A. Impact of human activities and climate change on vegetation around Hongjian nur lake in Northwestern China. *J. Desert Res.* **2010**, *30*, 831–836. (In Chinese)

32.　Tan, L.; Zhang, H.; Zhang, R.; Luo, Z.; Li, X.; Liu, P. Study on the landscape pattern change of Hongjiannao watershed in northern Shaanxi Province. *J. Xi'an Jiaotong Univ.* **2010**, *44*, 126–132. (In Chinese)

33.　Zhang, H.; Liu, P.; Li, X. Land use dynamic change of Hongjiannao watershed in northern shaanxi province. *Environ. Sci. Technol.* **2011**, *34*, 180–183. (In Chinese)

34.　Tang, K.; Wang, H.; Liu, C. Preliminary study of hongjiannao lake's variation and ecological water demand. *J. Nat. Resour.* **2003**, *18*, 304–309. (In Chinese)

35.　Liu, P.; Gan, W.; Zhang, R.; Tan, L. Quantitative analysis on water volume change and impacting factors for hongjiannao watershed in northern shaanxi province. *J. Xi'an Jiaotong Univ.* **2009**, *43*, 119–124. (In Chinese)

36.　Yang, L.; Huang, Q.; Wu, J.; Jia, Z. Influence factors and prediction on area change of lake hongjiannao. *J. Arid Land Resour. Environ.* **2014**, *28*, 74–78. (In Chinese)

37.　Zhao, N.; Ma, C.; Yang, Y. Water quality variation of lake hongjiannao and its driving force analysis from 1973 to 2013. *J. Lake Sci.* **2016**, *28*, 982–993. (In Chinese)

38.　Ma, B.; Wu, L.; Zhang, X.; Li, X.; Liu, Y.; Wang, S. Locally adaptive unmixing method for lake-water area extraction based on modis 250m bands. *Int. J. Appl. Earth Obs. Geoinf.* **2014**, *33*, 109–118. [CrossRef]

39.　Yin, L.; zhang, M.; Dong, J. Area variation and controlling factors of lake hongjian, mu us desert, china based on remote sensing techniques. *Geol. Bull. China* **2008**, *27*, 1151–1156. (In Chinese)

40.　Li, D.; Zhuo, J.; Wang, Z. Effect of human activities and climate change on the water surface area of hongjiannao lake. *J. Glaciol. Geocryol.* **2009**, *31*, 1110–1115. (In Chinese)

41.　Wang, J.; Qu, J.; Zhang, W. Extraction and monitoring of hongjiannao lake area in mu us sandy land based on mixed pixel decomposition of remote sensing data. *J. Desert Res.* **2011**, *31*, 558–562. (In Chinese)

42.　Liu, Y.; Yue, H. Analysis of hongjiannao lake area based on smmi. *Sci. Technol. Eng.* **2016**, *16*, 122–127. (In Chinese)

43.　Liu, Y.; Wu, L.; Yue, H. Monitoring of hongjiannao lake area based on landsat and hj imageries. *Geogr. Geo-Inf. Sci.* **2015**, *31*, 60–64. (In Chinese)

44.　Zhang, B.; Yang, L.; Ge, H.; Dong, W. Study on the countermeasures to alleviate the water ecological environment crisis. *Agric. Ltechnol.* **2013**, *33*, 41–42. (In Chinese)

45. Rubini, B.; Berezovikov, N.N. The fluctuation of breeding numbers of relict gull larus relictus onlake alakol (se kazakhstan): A review of surveys from 1968 to 2001. *Acrocephalus* **2002**, *23*, 185–188.

46. He, F.Q.; Ren, Y.-Q. Alternative choosing of breeding sites of those ordos relict gulls. *China Nat.* **2006**, *4*, 16–17. (In Chinese)

47. Liang, K. Quantifying streamflow variations in ungauged lake basins by integrating remote sensing and water balance modelling: A case study of the erdos larus relictus national nature reserve, china. *Remote Sens.* **2017**, *9*, 588. [CrossRef]

48. Allen, R.G.; Pereira, L.S.; Raes, D.; Smith, M. *Crop Evapotranspiration-Guidelines for Computing Crop Water Requirements-Fao Irrigation and Drainage Paper 56*; FAO: Rome, Italy, 1998; Volume 300, p. D05109.

49. Tucker, C.J.; Pinzon, J.E.; Brown, M.E.; Slayback, D.A.; Pak, E.W.; Mahoney, R.; Vermote, E.F.; El Saleous, N. An extended avhrr 8-km ndvi dataset compatible with modis and spot vegetation NDVI data. *Int. J. Remote Sens.* **2005**, *26*, 4485–4498. [CrossRef]

50. Holben, B.N. Characteristics of maximum-value composite images from temporal avhrr data. *Int. J. Remote Sens.* **1986**, *7*, 1417–1434. [CrossRef]

51. Piao, S.; Wang, X.; Ciais, P.; Zhu, B.; Wang, T.; Liu, J. Changes in satellite-derived vegetation growth trend in temperate and boreal eurasia from 1982 to 2006. *Glob. Chang. Biol.* **2011**, *17*, 3228–3239. [CrossRef]

52. Xu, H. Modification of normalised difference water index (NDWI) to enhance open water features in remotely sensed imagery. *Int. J. Remote Sens.* **2006**, *27*, 3025–3033. [CrossRef]

53. Mcfeeters, S.K. The use of the normalized difference water index (NDWI) in the delineation of open water features. *Int. J. Remote Sens.* **1996**, *17*, 1425–1432. [CrossRef]

54. Ji, L.; Zhang, L.; Wylie, B. Analysis of dynamic thresholds for the normalized difference water index. *Photogramm. Eng. Remote Sens.* **2009**, *75*, 1307–1317. [CrossRef]

55. Liu, C.; Zhang, D.; Liu, X.; Zhao, C. Spatial and temporal change in the potential evapotranspiration sensitivity to meteorological factors in china (1960–2007). *J. Geogr. Sci.* **2012**, *22*, 3–14. [CrossRef]

56. Keyantash, J.; Dracup, J.A. The quantification of drought: An evaluation of drought indices. *Bull. Am. Meteorol. Soc.* **2002**, *83*, 1167.

57. Van Den Broeke, M.; Bamber, J.; Ettema, J.; Rignot, E.; Schrama, E.; van de Berg, W.J.; van Meijgaard, E.; Velicogna, I.; Wouters, B. Partitioning recent greenland mass loss. *Science* **2009**, *326*, 984–986. [CrossRef] [PubMed]

58. Wei, F. *Modern Climatic Statistical Diagnosis and Prediction Techniques*, 2nd ed.; China Meteorological Press: Beijing, China, 2007.

59. Gibbs, P.H. Introduction to linear regression analysis. *Technometrics* **2012**, *25*, 2775–2776. [CrossRef]

60. Lee Rodgers, J.; Nicewander, W.A. Thirteen ways to look at the correlation coefficient. *Am. Stat.* **1988**, *42*, 59–66. [CrossRef]

61. Liang, K.; Bai, P.; Li, J.; Liu, C. Variability of temperature extremes in the yellow river basin during 1961–2011. *Quat. Int.* **2014**, *336*, 52–64. [CrossRef]

62. Liang, K.; Liu, S.; Bai, P.; Nie, R. The yellow river basin becomes wetter or drier? The case as indicated by mean precipitation and extremes during 1961–2012. *Theor. Appl. Climatol.* **2015**, *119*, 701–722. [CrossRef]

63. Hrachowitz, M.; Savenije, H.H.G.; Blöschl, G.; Mcdonnell, J.J.; Sivapalan, M.; Pomeroy, J.W.; Arheimer, B.; Blume, T.; Clark, M.P.; Ehret, U. A decade of predictions in ungauged basins (pub)—A review. *Hydrol. Sci. J.* **2013**, *58*, 1–58. [CrossRef]

64. Montanari, A.; Young, G.; Savenije, H.H.G.; Hughes, D.; Wagener, T.; Ren, L.L.; Koutsoyiannis, D.; Cudennec, C.; Toth, E.; Grimaldi, S. Panta rhei-everything flows: Change in hydrology and society-the iahs scientific decade 2013–2022. *Hydrol. Sci. J.* **2013**, *58*, 1256–1275. [CrossRef]